



Tree Physiology 36, 932–941
doi:10.1093/treephys/tpw027



Methods paper

Predictive models for radial sap flux variation in coniferous, diffuse-porous and ring-porous temperate trees

Aaron B. Berdanier^{1,2,5}, Chelcy F. Miniati³ and James S. Clark^{2,4}

¹University Program in Ecology, Duke University, Durham, NC 27708, USA; ²Nicholas School of the Environment, Levine Science Research Center A311, Duke University, Durham, NC 27708, USA; ³Coweeta Hydrologic Lab, USDA Forest Service, Southern Research Station, Otto, NC 28763, USA; ⁴Department of Statistical Science, Duke University, Durham, NC 27708, USA; ⁵Corresponding author (aaron.berdanier@gmail.com)

Received December 3, 2015; accepted March 15, 2016; handling Editor Nathan Phillips

Accurately scaling sap flux observations to tree or stand levels requires accounting for variation in sap flux between wood types and by depth into the tree. However, existing models for radial variation in axial sap flux are rarely used because they are difficult to implement, there is uncertainty about their predictive ability and calibration measurements are often unavailable. Here we compare different models with a diverse sap flux data set to test the hypotheses that radial profiles differ by wood type and tree size. We show that radial variation in sap flux is dependent on wood type but independent of tree size for a range of temperate trees. The best-fitting model predicted out-of-sample sap flux observations and independent estimates of sapwood area with small errors, suggesting robustness in the new settings. We develop a method for predicting whole-tree water use with this model and include computer code for simple implementation in other studies.

Keywords: hierarchical Bayes, plant hydraulics, radial profile, water use, wood anatomy.

Introduction

Predicting whole-tree water use requires models that accommodate the variation in sap flux between wood types and by depth into the tree. Estimates of whole-tree and ecosystem water use are often based on sap flux density measurements that are restricted to the outer portion of the xylem where much of the sap flux occurs. Radial variation in axial sap flux affects the scaling of these measurements to tree- or stand-levels (Edwards and Warwick 1984, Hatton et al. 1990, Wullschleger and King 2000, Nadezhdina et al. 2002). While it is clear that not all sapwood is functionally equal, a general model that allows upscaling by depth and xylem type is currently lacking in the literature (Phillips et al. 1996, Gebauer et al. 2008). In this article, we test models for the radial pattern of axial sap flux density (henceforth, radial profile) and generate predictive algorithms for their implementation in other settings.

Knowledge of the variation in radial profiles within and among trees has expanded in the last few decades. Generally, axial sap

flux density declines radially from the cambium until the transition to heartwood, where rates often approach zero (Čermák et al. 1992, Phillips et al. 1996, Taylor et al. 2002). Differences in radial profiles among trees are related to xylem anatomy (Phillips et al. 1996, Lüttschwager and Remus 2007, Tateshi et al. 2008), as well as conductivity (Ewers and Zimmermann 1984, Domec et al. 2005) and xylem cavitation or senescence (Mark and Crews 1973, Tyree and Zimmerman 2002). These patterns are connected to variation in canopy conductance (Hernandez-Santana et al. 2016). Analyses show differences among trees (Jiménez et al. 2000, Ford et al. 2004b, Cohen et al. 2008, Gebauer et al. 2008) and environments (Ford et al. 2004a, Kubota et al. 2005), although observations are often restricted to a few individuals, species or sites.

Like previous studies, we recognize three main wood types: non-porous or tracheid xylem, diffuse-porous xylem and ring-porous xylem (Panshin and de Zeeuw 1980). Non-porous xylem is a network of relatively small tracheid cells used for

water transport and structural support. Diffuse-porous xylem additionally contains large vessels that are randomly distributed throughout the wood, while ring-porous xylem has vessels bimodally distributed: larger diameter vessels are concentrated in the early-wood, and smaller diameter vessels are concentrated in the late-wood. Tracheid-bearing, non-porous conifers and diffuse-porous trees tend to have deep functional sapwood as well as low average specific conductivity due to small and short conduits. In contrast, while most of the conductance in ring-porous species is isolated to the outermost annual growth ring that contains functional early- and late-wood vessels, the late-wood vessels in older annuli are also functional (Čermák et al. 1992, Bush et al. 2010). Despite recognition of the differences in flow with xylem anatomy (McCulloh et al. 2010), few studies have tested whether radial profiles vary systematically across wood types.

Existing models of sap flux along radial profiles have different functional forms, goals and implementation. Most functions are continuous with depth into the xylem, although many (e.g., polynomial functions) do not have explicitly defined dimensions with respect to depth (Edwards and Warwick 1984, Gebauer et al. 2008). Some models use relative depth into the xylem (Oishi et al. 2008, Caylor and Dragoni 2009), while others use absolute depth (Cohen et al. 2008, Gebauer et al. 2008). Some models predict a maximum peak in flux beneath the cambium, while others require flux to monotonically decline with depth. Each of these models includes implicit assumptions about patterns in functioning sapwood area and water use with tree size.

Despite an increase in the number of models that could predict radial profiles of sap flux, researchers often use other approaches to scale sap flux measurements to whole trees or stands. Only 15% of published studies that we surveyed from the past 3 years that scaled-up with sap flux measurements ($n = 122$, see Table S1 available as Supplementary Data at *Tree Physiology* Online) used continuous radial profile models (and only 10% used nonlinear functions). The majority of the studies (58%) assumed homogenous flow throughout the xylem and the rest (27%) used a discrete, weighted-mean approach (Hatton et al. 1990). Studies that examine radial profiles often highlight the predictive opportunity of generalizable models (Delzon et al. 2004, Fiora and Cescatti 2006, Poyatos et al. 2007, Caylor and Dragoni 2009). However, few of the previous models are reused because they are difficult to implement, there is uncertainty about their predictive ability and calibration measurements may not be available for studies that are focused on other hypotheses besides radial variation. There is a need for transferrable models that can allow researchers to account for radial variation in axial sap flux density even when species- or site-specific observations are unavailable.

This study combines a taxonomically and anatomically diverse sap flux data set with a suite of models for predicting radial profiles to characterize variation across trees and wood types. Our data set includes observations of sap flux density by depth from

34 trees of 13 species from southeastern US forests. We use these data to compare different models and test the hypotheses that radial profiles differ by wood type and tree size. After assessing model fit and out-of-sample predictive ability with holdout observations and independent data, we develop a method for scaling-up independent flux observations from the outer xylem of comparable trees. As an illustrative example of applying these predictive models, we use the best-fitting model and sap flux observations from a forest in North Carolina to examine changes in water use with tree size. We include computer software for generating whole-tree flow estimates with other observations in Excel® and the R programming language as a supplement.

Materials and methods

Radial profile models

Whole-tree water flow rates can be modeled as the product of the average sap flux density in the sapwood, \bar{v} ($\text{g H}_2\text{O m}^{-2} \text{s}^{-1}$), and the sapwood area, A (m^2):

$$Q = \bar{v}A \quad (1)$$

This model requires an estimate of the average flux throughout the sapwood. If observations are constrained to the outer xylem and sap flux declines with depth into the tree, then this model will overestimate water flow (Delzon et al. 2004, Ford et al. 2004b). To include variation with depth, sap flux can be integrated across the stem (Edwards and Warwick 1984). Assuming radial symmetry, whole-tree water flow, Q ($\text{g H}_2\text{O s}^{-1}$), depends on the depth into the xylem from the cambium, x (m), along the tree radius, R (m), and a function for sap flux density by depth, $f(x;\theta)$ ($\text{g H}_2\text{O m}^{-2} \text{s}^{-1}$) that is conditional on shape parameters, θ :

$$Q = 2\pi \int_0^R (R-x)f(x;\theta)dx \quad (2)$$

Equations (1) and (2) are related to each other through the sapwood depth, S (m), where $A = \pi R^2 - \pi(R-S)^2$. The whole-tree flow can also be defined for the relative radial depth, $r = x/R$ (dimensionless), so that $Q = 2\pi R^2 \int_0^1 (1-r)f(r)dr$ (Caylor and Dragoni 2009). Models for $f(x)$ are frequently represented by modifications of probability functions, but they require proper dimensions (they must integrate to $\text{g H}_2\text{O s}^{-1}$). We compare four functions for the instantaneous sap flux density with depth that are similar to those applied by others (Table 1). All of these models are continuous and ultimately decay with depth into the xylem. One model (half-Gaussian) uses absolute depth into the xylem and requires sap flux density to decline from the cambium. Another model (beta) uses depth relative to the tree radius (0–1 instead of 0– R), which causes the functional sapwood depth to increase isometrically with tree size (since the radial profile expands with increasing radius) and sapwood area to increase proportional to the tree radius squared. Two models (beta and

Table 1. Models for the radial profile of sap flux density.

Model	Function, $f(x;\theta)$	Parameters, θ (name, units, prior constraint)
Half-Gaussian ¹	$Je^{-\beta x^2}$	J_1 (scale, $g\ m^{-2}\ s^{-1}$) β_1 (location, m^{-2})
Gaussian ²	$Je^{-\beta(x-\alpha)^2}$	J_2 (scale, $g\ m^{-2}\ s^{-1}$) α_2 (peak depth, m , >0) β_2 (location, m^{-2} , >0)
Gamma ³	$J(\beta x)^\alpha e^{-\beta x}$	J_3 (scale, $g\ m^{-2}\ s^{-1}$) α_3 (shape, dimensionless, >0) β_3 (rate, m^{-1} , >0)
Beta ⁴	$Jr^{\alpha-1}(1-r)^{\beta-1}$	J_4 (scale, $g\ m^{-2}\ s^{-1}$) α_4 (shape, dimensionless, >0) β_4 (shape, dimensionless, >1)

References with similar functions: ¹Bell et al. (2015), ²Ford et al. (2004b), ³Gebauer et al. (2008) and ⁴Caylor and Dragoni (2009).

gamma) are flexible for concave or convex shapes depending on the parameterization but differ in part because the gamma model represents absolute depth. These models represent different hypotheses for the form of radial profiles that we test with model comparison after fitting them with sap flux density observations.

Radial sap flux density data

Observations of sap flux density at depth (v_{ik}) were taken on 34 trees (i) from 13 species of tree wood types (k): 12 non-porous coniferous, 12 diffuse-porous hardwoods and 10 ring-porous hardwood trees (Table 2). Trees ranged in size from 10.1 to 65.8 cm diameter at breast height (DBH), with two to nine depth samples per tree depending on sapwood depth. Sapwood estimates from visual tree core examinations were collected for 28 of the trees to verify that thermocouples were in hydroactive sapwood. We used these data and data collected in the same area by Martin et al. (1998) (compiled in Falster et al. 2015) as an independent test of the model predictions of sapwood area. We also examined the assumption from the relative depth model (beta) that sapwood area scales with tree radius to a power of two with a slope test on a power function (Warton et al. 2006). The sap flux density data were collected between 2002 and 2009 for other studies, including analyses of whole-tree water use (Ford et al. 2004b), hydrological impacts of tree mortality (Ford and Vose 2007) and forest management influences on water budgets (Ford et al. 2011). Thermal dissipation probes (Lu et al. 2004) were used for all observations, although measurements for *Pinus* spp. were made with long probes (sensu Ford et al. 2004b) and the rest were made with variable length probes (sensu James et al. 2002). The probes had independent thermocouples that were inserted radially into the sapwood in 2 cm increments starting at 1 cm at ~1.3 m above the ground. Estimates of v were based on the empirical thermal dissipation calibration from Granier (1985). The probes were 1 cm in length to minimize velocity gradients across the probe and to ensure that each probe was fully in conductive xylem (Renninger

Table 2. Measured species, numbers of trees and size ranges for each wood type.

Species	N	DBH range (m)	Reference
Non-porous coniferous			
<i>Pinus echinata</i> Mill.	1	0.410	Ford et al. 2004b
<i>Pinus elliotii</i> Engelm.	1	0.476	
<i>Pinus palustris</i> Mill.	4	0.314–0.568	
<i>Pinus taeda</i> L.	4	0.284–0.338	
<i>Tsuga canadensis</i> L.	2	0.320–0.512	Ford and Vose (2007)
Diffuse-porous hardwoods			
<i>Acer rubrum</i> L.	2	0.257–0.322	C.F. Miniati, unpublished data
<i>Betula lenta</i> L.	4	0.139–0.301	C.F. Miniati, unpublished data
<i>Liriodendron tulipifera</i> L.	3	0.243–0.610	Ford et al. (2011)
<i>Platanus occidentalis</i> L.	3	0.140–0.360	C.F. Miniati, unpublished data
Ring-porous hardwoods			
<i>Carya</i> spp.	2	0.332–0.338	Ford et al. (2011)
<i>Fraxinus pennsylvanica</i> Marshall	4	0.095–0.324	C.F. Miniati, unpublished data
<i>Quercus rubra</i> L.	2	0.425–0.427	Ford et al. (2011)
<i>Robinia pseudoacacia</i> L.	2	0.193–0.323	C.F. Miniati, unpublished data

and Schäfer 2012). We only included trees that had at least three full observation days; the average observation period across trees was 16 days. Because the data were collected on different days and contain different numbers of days for most trees, we averaged the midday observations for each tree at each depth and then aggregated across available observation days, resulting in 144 unique tree-depth observations that represent the average midday sap flux density.

Model fitting and selection

We fit observations of sap flux density to each of the functions in Table 1 with a Bayesian hierarchical model. The observations (v_{ik}) were lognormally distributed around the model-predicted flux value (\hat{v}_{ik}) with an observation error (σ^2) that had an inverse gamma (IG) distribution. The parameters of the function (θ_k) had a multivariate normal (MVN) distribution. We included random effects for each individual (δ_i) to accommodate differences among trees in the absolute magnitude of average sap flux density. For one observation:

$$\ln(v_{ik}) \sim N(\ln(\hat{v}_{ik}), \sigma^2)$$

$$\ln(\hat{v}_{ik}) = \ln(f(x_{ik}; \theta_k)) + \delta_i$$

$$\theta_k \sim \text{MVN}(0, \Sigma)$$

$$\delta_i \sim N(0, \tau^2)$$

$$\sigma^2 \sim \text{IG}(u_1, u_2)$$

$$\tau^2 \sim \text{IG}(v_1, v_2)$$

where Σ is the prior covariance on the function parameters and u_1 , v_1 , u_2 and v_2 are prior shape and scale parameters for the observation error and random individual effects. Prior distributions for the function parameters differed among the models and were defined to maintain biologically realistic responses (e.g., positive skew in the beta model; see Table 1 for all prior constraints).

For each function, we fit two versions, one where each wood type group had independent function parameters (fitted simultaneously, hereafter referenced with a '-type' suffix) and another where all trees had global function parameters (excluding k subscripts above), resulting in eight independent models for comparison. We estimated all parameters (function parameters, observation error and random effects) with Gibbs sampling in the R program (R Development Core Team 2015). When possible, parameters were sampled directly from conditional posterior distributions. The remaining parameters were sampled with a Metropolis–Hastings algorithm. Each model was fit with 70,000 iterations. We excluded the first 20,000 iterations before summarizing the posterior distribution for each parameter to ensure parameter convergence.

Comparisons among the models allowed us to test the hypothesis that radial profiles differed among wood types (i.e., if a model with distinct function parameters for each wood type fit better than a model with common function parameters) and to identify model forms that performed better than others. We used three criteria for model selection: the predictive score (PS) (Gneiting and Rafferty 2007), deviance information criterion (DIC) (Spiegelhalter et al. 2002) and the root mean square predictive error (RMSPE; $\text{g H}_2\text{O m}^{-2} \text{s}^{-1}$). The PS assesses predictive ability by rewarding predictive accuracy and penalizing over-confident predictions; high values are preferred. Deviance information criterion is a model selection criterion that rewards a good fit but penalizes model complexity; low values are preferred. Root mean square predictive error and PS were generated with a 10-fold cross-validation procedure where the original data were partitioned to exclude data from three trees (one from each wood type) in each fold. Holdout tree selection was done without replacement so each fold contained a unique testing sample, producing out-of-sample predictions for 30 trees across models. For each testing sample, the model was refit with 7000 iterations and the posterior mean prediction (excluding a 2000 sample burn-in) was compared with the observation for predictive assessment. This cross-validation allowed us to assess the out-of-sample predictive ability of each model, as a measure of relative performance with new trees.

Predicting whole-tree water use

Predictions of flow rates on new trees require a correction factor to scale the sap flux density from the outer xylem to the whole tree. We generalized the approach used by Paudel et al. (2012) to accommodate nonlinear radial profiles by calculating the ratio of the predicted whole-tree sap flow ($g_{\text{all}} \text{s}^{-1}$) and the predicted

flow in the measured portion ($g_{\text{meas}} \text{s}^{-1}$), which are both found by integrating Eq. (2). With new observations of sap flux density on independent trees, \tilde{v} ($\text{g m}^{-2} \text{s}^{-1}$), measured over a given portion of the xylem [a, b], this correction factor is:

$$c = \frac{\int_0^R (R-x)f(x;\theta)dx}{\int_a^b (R-x)f(x;\theta)dx} \quad (3)$$

Because this correction factor is relative to the integral for the entire profile, the radial profile predictions are insensitive to possible linear deviations in flux due to probe calibration (Bush et al. 2010, Steppe et al. 2010, Renninger and Schäfer 2012, Sun et al. 2012).

The observed sap flux density is then scaled to the whole-tree flow rate, \tilde{Q} (g s^{-1}), with a modification of Eq. (1) that includes the new sap flux observation, the area of the measured portion, A_{meas} (m^2), and the correction factor:

$$\tilde{Q} = \tilde{v}A_{\text{meas}}c \quad (4)$$

Given the parameters of the function (θ) and new sap flux observations (\tilde{v}), estimates of whole-tree water use can be made with probe length and the tree size information. Additionally, the integrals for all of the models can be solved analytically, so that a tractable algorithm can be written to generate predictions (see Methods available as Supplementary Data at *Tree Physiology* Online). Using a similar procedure, we calculated the sapwood depth that accounted for 95% of the predicted whole-tree flow (an estimate for the functional sapwood depth) with the fitted parameters across tree sizes and calculated the expected functional sapwood areas for comparison with the sapwood area measurements.

We made predictions of whole-tree water use for 66 trees in a mixed hardwood stand of the Duke Forest (Orange County, NC, USA). All trees were monitored continuously between May and October 2013. Sap flux density observations were collected at 10-min intervals (and then aggregated to hourly averages) from each tree with 2 cm thermal dissipation probes, all installed into the xylem at ~ 1.3 m above the ground. Trees ranged in size from 10.8 to 72.3 cm DBH and were from 10 species (6 *Acer rubrum* L., 8 *Carya glabra* Miller, 8 *Carya tomentosa* Sarg., 4 *Fraxinus americana* L., 8 *Liquidambar styraciflua* L., 6 *Liriodendron tulipifera* L., 6 *Pinus taeda* L., 7 *Quercus alba* L., 7 *Quercus falcata* Michx. and 6 *Ulmus alata* Michx.). For each tree (i) of each species (s), we predicted instantaneous whole-tree water use ($\text{g H}_2\text{O s}^{-1}$) with the correction factor from the best-fitting model, integrated water use rates to a daily total (Q_{is} , $\text{kg H}_2\text{O day}^{-1}$) and took the average water use rate across days when the average daily solar radiation was $>50 \text{ W m}^{-2}$ (excluding cloudy and rainy days). We estimated the relationship between individual tree size and average water use with a linear mixed-effects model, $\ln(Q_{\text{is}}) = Q_0 + c$

$\ln(D_{is}) + d_s + e_{is}$, where D_{is} is the DBH of an individual, Q_0 is the log normalization constant, c is the power exponent, d_s is a species random effect and e_{is} are normally distributed errors, fitted with the 'lmer' function in R (Bates et al. 2014).

Results

Among all models, the gamma-type model (with specific parameters for each wood type) generated the best predictions both in and out of sample, with a RMSPE of $3.3 \text{ g m}^{-2} \text{ s}^{-1}$. Models for sap flux density with depth that included wood-type-specific parameters outperformed the models that did not identify wood types (Table 3). Among the models that included wood-type-specific parameters, the models parameterized for absolute depth from the cambium outperformed the model with relative depth into the tree. Predictions for all models showed some divergence at low sap flux densities, although the absolute prediction errors here were lower than those at higher values (Figure 1). For all models, the PS and out-of-sample predictive error were the same, and generally agreed with the DIC rankings.

Fitted parameters from the gamma-type model differed across wood types (Figure 2). For this model, the shape parameter controls the curvature and the rate parameter controls the decline with depth. The scale parameter controls the intensity above zero but has no influence on predictions for new trees (see Methods available as Supplementary Data at *Tree Physiology* Online). Differences in these fitted parameters across wood types and their combinations thus produced distinct patterns in the predicted radial profiles (Figure 3). Across wood types, the shape parameters declined from non-porous conifer to diffuse-porous hardwood to ring-porous hardwood. Non-porous conifer trees had a peak that was slightly behind the cambium (a pattern observed in the raw data for two-thirds of the conifer trees), while ring- and diffuse-porous hardwood trees peaked close to the edge because of their low shape parameter values (as the shape parameter approaches zero, this model reduces to a negative exponential). The rate parameter was higher in the ring-porous hardwood trees compared with the non-porous

Table 3. Model selection results, sorted by PS. The best model is highlighted in bold. Models that include parameters for each wood type include '-type' in the name.

Model	PS	DIC	RMSPE	Depth into the xylem
Gamma-Type	-0.38	341	3.27	Absolute
Half-Gaussian-type	-0.51	352	3.40	Absolute
Gamma	-0.53	351	4.81	Absolute
Gaussian-type	-0.57	363	3.47	Absolute
Beta-Type	-0.59	363	3.78	Relative
Beta	-0.63	370	4.40	Relative
Half-Gaussian	-0.64	370	4.54	Absolute
Gaussian	-0.66	373	4.55	Absolute

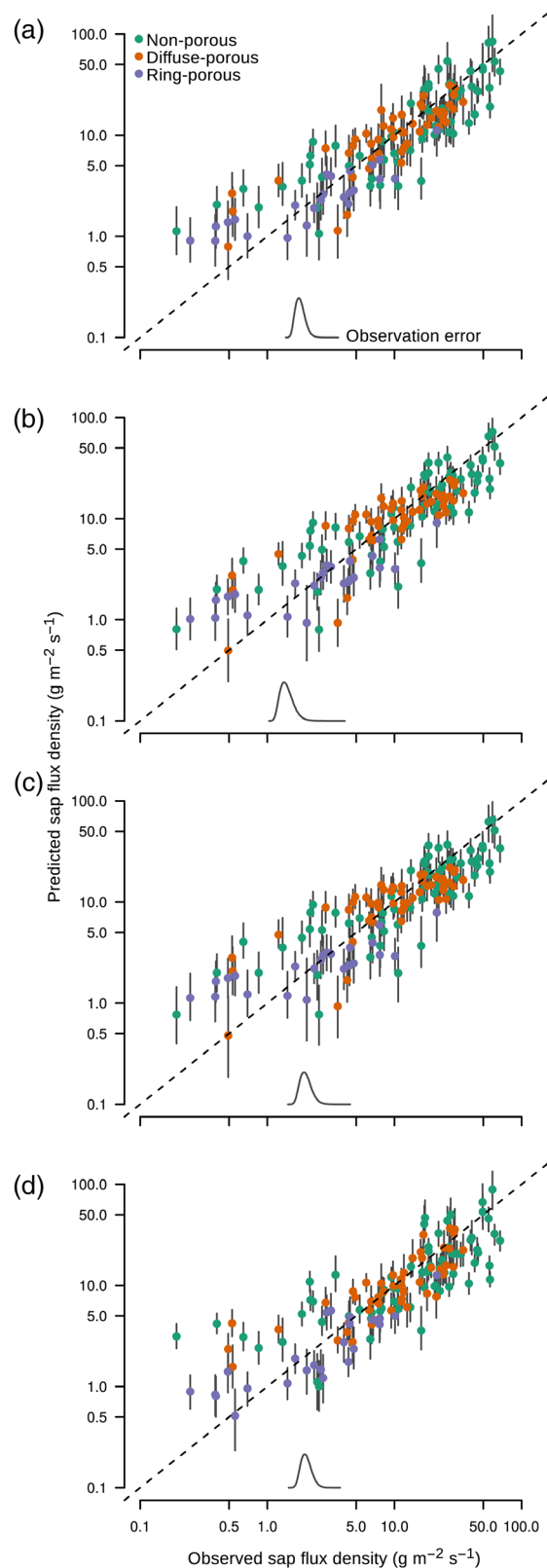


Figure 1. Predictions of sap flux density observations (mean and 95% credible intervals) for models that included wood-type-specific parameters, sorted top to bottom by model selection. Different wood types are identified by shading and the posterior density of the observation error (σ^2) is shown on the horizontal axis. (a) gamma-type, (b) half-Gaussian-type, (c) Gaussian-type and (d) beta-type.

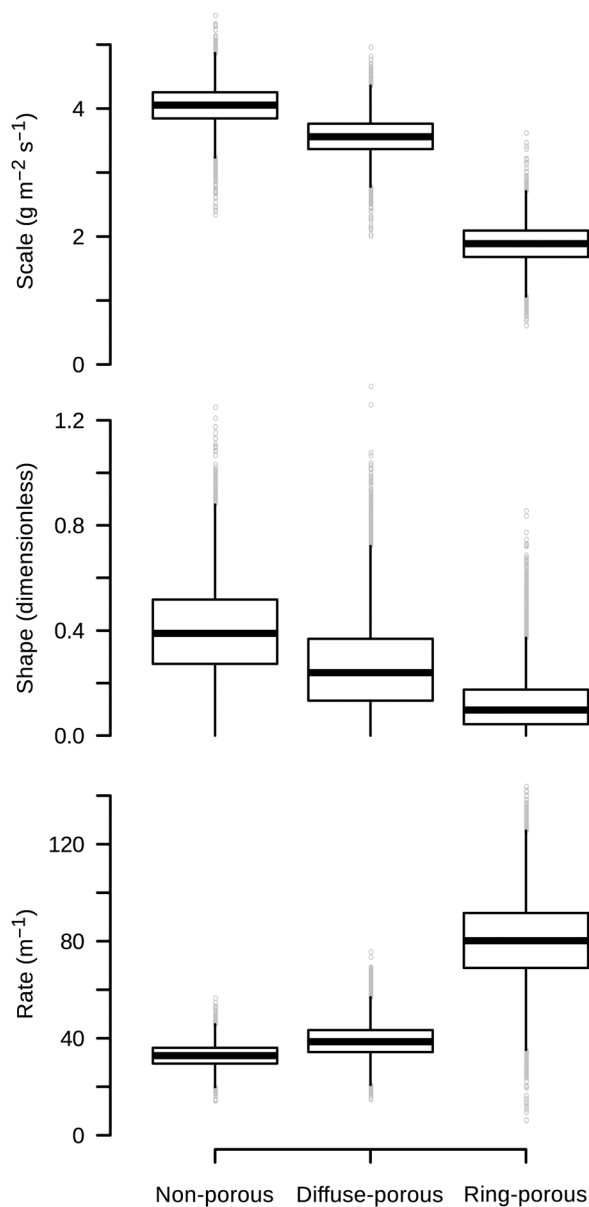


Figure 2. Posterior parameter estimates for the gamma-type model (the best-fitting model) across wood types.

coniferous and diffuse-porous hardwood trees, which were not different. This caused ring-porous trees to show rapid declines in sap flux over the first few centimeters.

The poor performance of the relative depth models and the importance of accounting for wood type can be explained in part by inconsistencies between model assumptions and observations of sapwood area. Across trees, sapwood area scaled with tree radius by a power of 1.75 (95% confidence interval: 1.53–1.96) and was different from two, based on a slope test with log-transformed values ($F = 5.45$, $P_{\text{slope}=2} = 0.02$). The independent observations of sapwood area were comparable to the predictions from the gamma-type model for the functional sapwood area (Figure 4), with clear separation across xylem

types, indicating additional consistency between model predictions and field observations.

We used the gamma-type model to generate estimates of whole-tree water use with observations of sap flux density from other trees (Figure 5). Differences in the radial profiles and size among trees led to variation in whole-tree water use rates (Figure 6). Including species random effects, the average daily water use increased with tree diameter by a power of 1.06 ± 0.11 (mean \pm SE). This mixed-effects model fit the data better than a linear model on log-transformed data without species effects, based on a likelihood ratio test ($\chi^2 = 5.04$, $P = 0.02$). The correlation between the observed and average predicted values from the mixed-effects model was 0.87. Species differences created large discrepancies in the predicted water use at large diameters.

Discussion

We found that predictions for the average radial profile of sap flux density were dependent on wood type but independent of tree size. Across trees, models that included parameters for non-porous coniferous, diffuse-porous and ring-porous wood types and were based on absolute depth into the xylem provided a superior fit to our data set. The gamma-type model generated the best predictions (Figure 1). This model is flexible for asymmetry in the decline with depth. The response for ring-porous trees was extremely peaked (close to a negative exponential response), while diffuse-porous trees showed a shallower decline with depth and coniferous trees had curvature with a peak that was beneath the cambium (Figure 3).

Differences among the radial profiles (Figures 2 and 3) in the best-fitting model emphasize the influence of wood type and xylem anatomy on whole-tree water use. Ring-porous trees have larger xylem conduits but have stem- and leaf-specific conductivities that are comparable to diffuse-porous and coniferous trees because of differences in hydroactive sapwood across wood types (McCulloh et al. 2010). For ring-porous trees in particular, much of the sap flux is restricted to the outer annual growth rings (Ellmore and Ewers 1986, Granier et al. 1994), which produces a strongly peaked radial profile (Gebauer et al. 2008). In contrast, xylem conduits near the cambium in non-porous conifer trees can have unopened bordered pits that restrict flow (Mark and Crews 1973). When combined with smaller xylem conduits and bordered pit closure toward the pith (Taylor et al. 2002, Domec et al. 2005), many conifer trees show a curved radial profile with a peak below the cambium (Čermák et al. 1992, Ford et al. 2004b, Krauss and Dauberstein 2010).

While the other models did not perform as well as the gamma-type model with these data, some still offered reasonable predictions. The second best predictive function was the half-Gaussian-type model. This model generated similar predictive

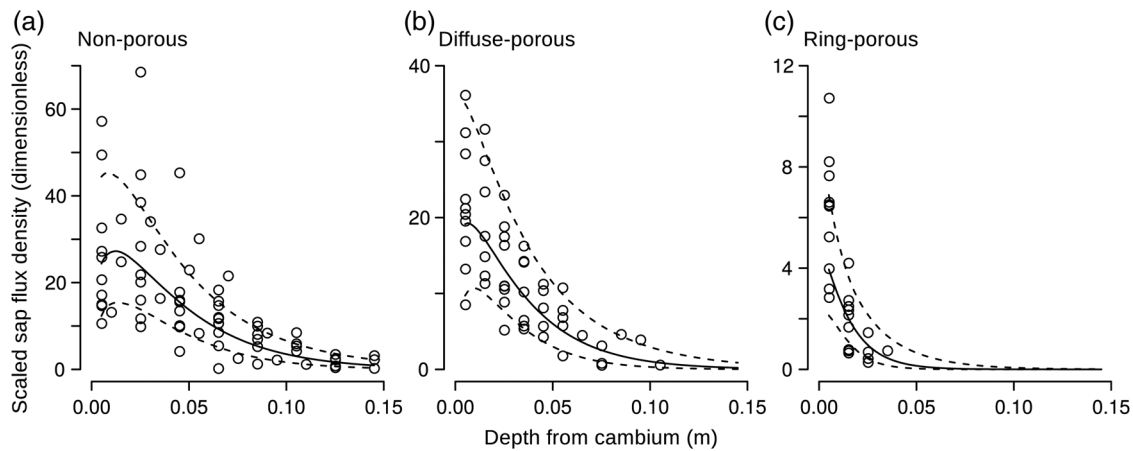


Figure 3. Predictions of the radial profile of sap flux density with depth for each wood type from the gamma-type model. Solid lines are the posterior mean of the fitted model and dashed lines show the 95% credible interval. The data for sap flux density are normalized for plotting by subtracting the posterior individual random effects (δ_i). (a) Non-porous, (b) diffuse porous and (c) ring porous.

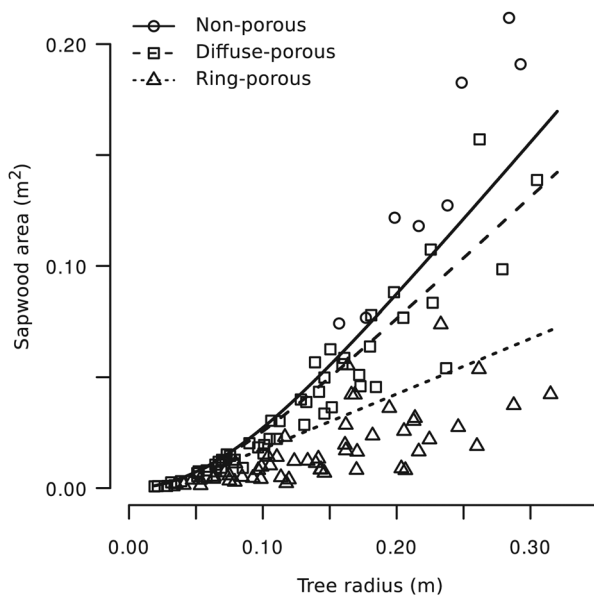


Figure 4. Observations (points) and predictions (lines) of sapwood area versus tree radius in non-porous (circles), diffuse-porous (squares) and ring-porous (triangles) trees. Data include trees used to parameterize the radial profile models ($n = 28$) and observations from Martin et al. (1998) ($n = 87$). Predictions for each wood type are average estimates for the area with 95% of functional sapwood from the gamma-type model.

errors to the gamma-type model (Table 3) and performed better than the similar Gaussian-type model, possibly because of model simplicity. The only difference between the Gaussian and half-Gaussian functions was the inclusion of a location parameter. The fitted values for this parameter across wood types were extremely low and frequently approached zero, leading the predictions between these two models to be similar on average but with one less parameter in the half-Gaussian model.

Across the range of tree sizes measured here, the models that represented the radial pattern of sap flux density as a function of absolute depth from the cambium provided better predictions

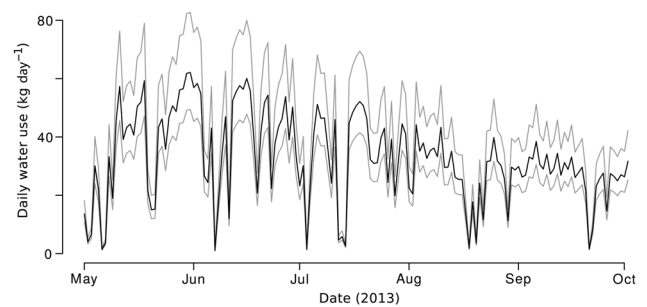


Figure 5. Example predictions for daily whole-tree water use ($kg\ H_2O\ day^{-1}$) calculated with the parameters from the gamma-type model for a *L. tulipifera* tree (DBH = 0.51 m) in the Duke Forest, Orange County, NC, USA. The solid lines show the mean and the gray lines show the 95% predictive interval.

than those based on relative depth into the tree. This finding suggests that, as trees increase in size, the older xylem becomes progressively less conductive and the newer xylem performs similarly to the former outer xylem. This prediction is consistent with recent observations connecting radial variation in sap flux with canopy variation in stomatal conductance (Hernandez-Santana et al. 2016). Models based on relative depth into the whole tree are not flexible for a range of size classes because heartwood formation is a cumulative process. Even if the hydroactive sapwood depth increases gradually with tree size, the fraction of sapwood often declines as size increases (Yang and Hazenberg 1991, Sellin 1994), which matches our observation that sapwood area scales with a power of less than two on average, lower than previously hypothesized values (Shinozaki et al. 1964, West et al. 1999) but consistent with other estimates (Meinzer et al. 2005). The sapwood observations can be simulated with our fitted radial profiles; our independent predictions of functional sapwood area from the gamma-type model generally matched the observations and clearly delineated differences among xylem types (Figure 4).

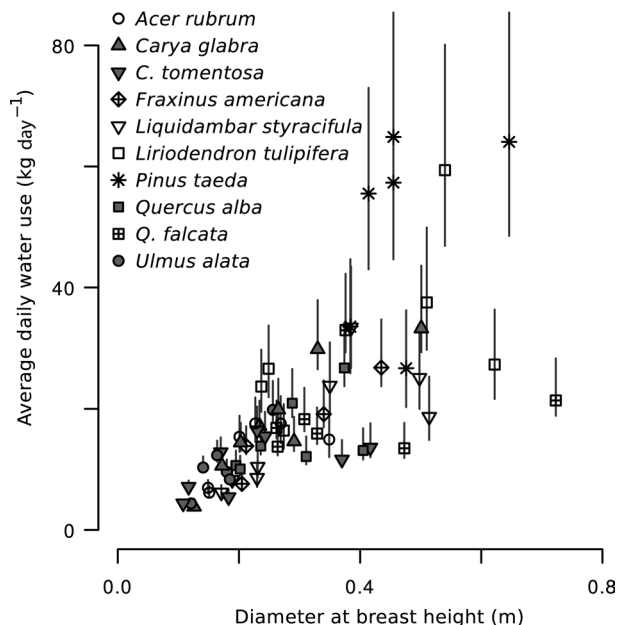


Figure 6. Estimates of average daily water use ($\text{kg H}_2\text{O day}^{-1}$) increase with diameter at breast height (m) for trees in the Duke Forest, Orange County, NC, USA. Species are identified with different symbols and vertical bars show 95% prediction intervals.

The functions presented here are based on absolute depth into the tree and the whole-tree radius. They can accommodate observations of sapwood area if they are available (see Materials available as Supplementary Data at *Tree Physiology* Online), but do not require them. This functional definition of the sapwood boundary is based on the empirical decline of sap flux density with depth and is pragmatic for prediction on new trees. While profiles based on relative depth into the sapwood (as opposed to the whole tree) could provide similar responses to the absolute functions (Oishi et al. 2008), they still depend on estimates of the heartwood transition from allometric equations or measurements of wood color or water content (Taylor et al. 2002, Meinzer et al. 2005, Poyatos et al. 2007), which can be difficult to measure and may not directly delineate the hydroactive sapwood area (Cermak and Nadezhkina 1998, Poyatos et al. 2007, Molina et al. 2016).

Our fitted models can generate predictions for trees that are similar to those examined here (Figure 5). We produced estimates of whole-tree water use for a diverse population of trees in a mixed temperate forest, covering a broad range of size classes and species (Figure 6). Our estimates of average water use are lower than those from studies that do not account for radial variation in sap flux density (Enquist et al. 1998, Wullschlegel et al. 1998) but are comparable to other studies that included radial declines in axial sap flux density, including another study in the Southern Appalachian Mountains with similar species (Ford et al. 2011) and observations from other temperate forest ecosystems (Meinzer et al. 2005, von Allmen et al. 2012). These whole-tree estimates suggest a lower scaling

exponent with tree diameter than previously reported, driven in part by differences among trees in functional sapwood area for a given size (Figure 4).

There are still limits to the applicability of our estimated parameters. First, in this analysis, we assume that the average midday radial profile is representative of most conditions for the trees during peak flow times, which should produce reliable estimates of daily water use. We did not consider variation in the fitting parameters diurnally or with environmental changes. Previous analyses have demonstrated that sap flux density patterns with depth can change throughout a season, for example due to changes in light or moisture (Ford et al. 2004a, Fiora and Cescatti 2006). We did not include these complexities because the data used here were collected from a variety of sites, often without colocated environmental data, and on different dates. Future studies could build environmental dependence into the shape parameters with additional hierarchical structure and could use the posterior parameter estimates reported here as prior information. Additionally, our data set is restricted to trees that are common in Southeastern US forests. If the parameters for the absolute depth model depend on xylem age, then our parameter estimates may not be representative for trees with different diameter increments (e.g., across diverse landscapes or in different biomes). However, the best-fitting model was able to accurately predict sap flux observations out-of-sample with small errors, suggesting robustness in new settings. We have also included the code for fitting model parameters with new radial profile data available as Supplementary Data at *Tree Physiology* Online. The fitted model, along with the algorithms that we have included as Supplementary Data at *Tree Physiology* Online, will be useful for translating observations of sap flux density to whole-tree water use in ecophysiological studies on a range of topics, including drought response and irrigation monitoring (Hernandez-Santana et al. 2016, Molina et al. 2016).

Conclusions

We have analyzed general models for the radial profile of sap flux density that can be used to calculate whole-tree water use with observations from independent sap flux probes. The model with the best performance is based on differences among wood types that represent functional differences in xylem anatomy. It provides reasonable predictions of sap flux density with depth both in and out of sample. For future studies, if sap flux observations with depth are available, the computer code included as Materials available as Supplementary Data at *Tree Physiology* Online can be used to generate new parameter estimates. If site- or species-specific observations of sap flux with depth are unavailable (as we often find), these Materials can provide reasonable estimates for comparable trees with easily collected morphological information and our fitted parameters. Predictions of whole-tree water

flux only require independent measurements of sap flux density across some radial interval in the xylem, the radius of the tree at the measurement height without bark and a general wood-type classification. The R functions additionally include measurements of uncertainty. These models will be useful for scaling sap flux density observations from new trees and estimating whole tree and stand transpiration.

Supplementary data

Supplementary data for this article are available at [Tree Physiology Online](#).

Acknowledgments

We are grateful to the Oren Lab at Duke University for loaning data loggers and appreciate helpful comments and suggestions from Matthew Kwit, Bijan Seyednasrollah and Bradley Tomasek.

Conflict of interest

None declared.

Funding

This research was supported by Coweeta Hydrologic Laboratory, US Department of Agriculture Forest Service and Southern Research Station, and the Coweeta Long Term Ecological Research project funded by National Science Foundation grant DEB-0823293. The use of trade or firm names in this publication is for reader information and does not imply endorsement by the US Department of Agriculture of any product or service.

References

- Bates D, Maechler M, Bolker B, Walker S (2014) lme4: linear mixed-effects models using Eigen and S4. R package version 1.1-6. <http://CRAN.R-project.org/package=lme4> (6 November 2014, date last accessed).
- Bell DM, Ward EJ, Oishi AC, Oren R, Flikkema PG, Clark JS (2015) A state-space modeling approach to estimating canopy conductance and associated uncertainties from sap flux density data. *Tree Physiol* 35:792–802.
- Bush SE, Hultine KR, Sperry JS, Ehleringer JR (2010) Calibration of thermal dissipation sap flow probes for ring- and diffuse-porous trees. *Tree Physiol* 30:1545–1554.
- Caylor KK, Dragoni D (2009) Decoupling structural and environmental determinants of sap velocity: part I. Methodological development. *Agric For Meteorol* 149:559–569.
- Cermak J, Nadezhdina N (1998) Sapwood as the scaling parameter-defining according to xylem water content or radial pattern of sap flow? *Ann For Sci* 55:509–521.
- Čermák J, Cienciala E, Kučera J, Hällgren J-E (1992) Radial velocity profiles of water flow in trunks of Norway spruce and oak and the response of spruce to severing. *Tree Physiol* 10:367–380.
- Cohen Y, Cohen S, Cantuarias-Aviles T, Schiller G (2008) Variations in the radial gradient of sap velocity in trunks of forest and fruit trees. *Plant Soil* 305:49–59.
- Delzon S, Sartore M, Granier A, Loustau D (2004) Radial profiles of sap flow with increasing tree size in maritime pine. *Tree Physiol* 24:1285–1293.
- Domec J-C, Meinzer FC, Gartner BL, Woodruff D (2005) Transpiration-induced axial and radial tension gradients in trunks of Douglas-fir trees. *Tree Physiol* 26:275–284.
- Edwards WRN, Warwick NWM (1984) Transpiration from a kiwifruit vine as estimated by the heat pulse technique and the Penman-Monteith equation. *N Z J Agric Res* 27:537–543.
- Ellmore GS, Ewers FW (1986) Fluid flow in the outermost xylem increment of a ring-porous tree, *Ulmus americana*. *Am J Bot* 73:1771–1774.
- Enquist BJ, Brown JH, West GB (1998) Allometric scaling of plant energetics and population density. *Nature* 395:163–165.
- Ewers FW, Zimmermann MH (1984) The hydraulic architecture of eastern hemlock (*Tsuga canadensis*). *Can J Bot* 62:940–946.
- Falster DS, Duursma RA, Ishihara MI et al. (2015) BAAD: a Biomass And Allometry Database for woody plants. *Ecology* 96:1445–1445.
- Fiora A, Cescatti A (2006) Diurnal and seasonal variability in radial distribution of sap flux density: implications for estimating stand transpiration. *Tree Physiol* 26:1217–1225.
- Ford CR, Vose JM (2007) *Tsuga canadensis* (L.) Carr. mortality will impact hydrologic processes in southern Appalachian forest ecosystems. *Ecol Appl* 17:1156–1167.
- Ford CR, Goranson CE, Mitchell RJ, Will RE, Teskey RO (2004a) Diurnal and seasonal variability in the radial distribution of sap flow: predicting total stem flow in *Pinus taeda* trees. *Tree Physiol* 24:951–960.
- Ford CR, McGuire MA, Mitchell RJ, Teskey RO (2004b) Assessing variation in the radial profile of sap flux density in *Pinus* species and its effect on daily water use. *Tree Physiol* 24:241–249.
- Ford CR, Laseter SH, Swank WT, Vose JM (2011) Can forest management be used to sustain water-based ecosystem services in the face of climate change? *Ecol Appl* 21:2049–2067.
- Gebauer T, Horna V, Leuschner C (2008) Variability in radial sap flux density patterns and sapwood area among seven co-occurring temperate broad-leaved tree species. *Tree Physiol* 28:1821–1830.
- Gneiting T, Raftery AE (2007) Strictly proper scoring rules, prediction, and estimation. *J Am Stat Assoc* 102:359–378.
- Granier A (1985) Une nouvelle méthode pour la mesure du flux de sève brute dans le tronc des arbres. *Ann For Sci* 42:193–200.
- Granier A, Anfodillo T, Sabatti M, Cochard H, Dreyer E, Tomasi M, Valentini R, Bréda N (1994) Axial and radial water flow in the trunks of oak trees: a quantitative and qualitative analysis. *Tree Physiol* 14:1383–1396.
- Hatton TJ, Catchpole EA, Vertessy RA (1990) Integration of sapflow velocity to estimate plant water use. *Tree Physiol* 6:201–209.
- Hernandez-Santana V, Fernández JE, Rodríguez-Dominguez CM, Romero R, Diaz-Espejo A (2016) The dynamics of radial sap flux density reflects changes in stomatal conductance in response to soil and air water deficit. *Agric For Meteorol* 218–219:92–101.
- James SA, Clearwater MJ, Meinzer FC, Goldstein G (2002) Heat dissipation sensors of variable length for the measurement of sap flow in trees with deep sapwood. *Tree Physiol* 22:277–283.
- Jiménez MS, Nadezhdina N, Čermák J, Morales D (2000) Radial variation in sap flow in five laurel forest tree species in Tenerife, Canary Islands. *Tree Physiol* 20:1149–1156.
- Krauss KW, Dauberstein JA (2010) Sapflow and water use of freshwater wetland trees exposed to saltwater incursion in a tidally influenced South Carolina watershed. *Can J For Res* 40:525–535.
- Kubota M, Tenhunen J, Zimmermann R, Schmidt M, Adiku S, Kakubari Y (2005) Influences of environmental factors on the radial profile of sap flux density in *Fagus crenata* growing at different elevations in the Naeba Mountains, Japan. *Tree Physiol* 25:525–556.
- Lu P, Urban L, Zhao P (2004) Granier's thermal dissipation probe (TDP) method for measuring sap flow in trees: theory and practice. *Acta Bot Sin* 46:631–646.

- Lüttschwager D, Remus R (2007) Radial distribution of sap flux density in trunks of a mature beech stand. *Ann For Sci* 64:431–438.
- Mark WR, Crews DL (1973) Heat-pulse velocity and bordered pit condition in living Engelmann spruce and Lodgepole pine trees (*Picea engelmannii*, *Pinus contorta*). *Forest Sci* 19:291–296.
- Martin JG, Kloeppel BD, Schaefer TL, Kimbler DL, McNulty SG (1998) Aboveground biomass and nitrogen allocation of ten deciduous southern Appalachian tree species. *Can J For Res* 28:1648–1659.
- McCulloh K, Sperry JS, Lachenbruch B, Meinzer FC, Reich PB, Voelker S (2010) Moving water well: comparing hydraulic efficiency in twigs and trunks of coniferous, ring-porous, and diffuse-porous saplings from temperate and tropical forests. *New Phytol* 186:439–450.
- Meinzer FC, Bond BJ, Warren JM, Woodruff DR (2005) Does water transport scale universally with tree size? *Funct Ecol* 18:558–565.
- Molina AJ, Aranda X, Carta G, Llorens P, Romero R, Savé R, Biel C (2016) Effect of irrigation on sap flux density variability and water use estimate in cherry (*Prunus avium*) for timber production: Azimuthal profile, radial profile and sapwood estimation. *Agric Water Manag* 164:118–126.
- Nadezhdina N, Čermák J, Ceulemans R (2002) Radial patterns of sap flow in woody stems of dominant and understory species: scaling errors associated with positioning of sensors. *Tree Physiol* 22:907–918.
- Oishi AC, Oren R, Stoy PC (2008) Estimating components of forest evapotranspiration: a footprint approach for scaling sap flux measurements. *Agric For Meteorol* 148:1719–1732.
- Panshin AJ, de Zeeuw C (1980) *Textbook of wood technology*, 4th edn. McGraw-Hill Book Co., New York, pp 127–200.
- Paudel I, Kanety T, Cohen S (2012) Inactive xylem can explain differences in calibration factors for thermal dissipation probe sap flow measurements. *Tree Physiol* 33:986–1001.
- Phillips N, Oren R, Zimmerman R (1996) Radial patterns of xylem sap flow in non-, diffuse- and ring-porous tree species. *Plant Cell Environ* 19:983–990.
- Poyatos R, Čermák J, Llorens P (2007) Variation in the radial patterns of sap flux density in pubescent oak (*Quercus pubescens*) and its implications for tree and stand transpiration measurements. *Tree Physiol* 27:537–548.
- R Development Core Team (2015) *R: a language and environment for statistical computing*. R Foundation for Statistical Computing, Vienna, Austria.
- Renninger HJ, Schäfer KVR (2012) Comparison of tissue heat balance- and thermal dissipation-derived sap flow measurements in ring-porous oaks and a pine. *Front Plant Sci* 3:103. doi:10.3389/fpls.2012.00103
- Sellin A (1994) Sapwood–heartwood proportion related to tree diameter, age, and growth rate in *Picea abies*. *Can J For Res* 24:1022–1028.
- Shinozaki K, Yoda K, Hozumi K, Kira T (1964) A quantitative analysis of plant form—the pipe model theory. I. Basic analyses. *Jpn J Ecol* 14:97–105.
- Spiegelhalter DJ, Best NG, Carlin BP, van der Linde A (2002) Bayesian measures of model complexity and fit. *J R Stat Soc B* 64:583–639.
- Steppe K, De Pauw DJW, Doody TM, Tesky RO (2010) A comparison of sap flux density using thermal dissipation, heat pulse velocity and heat field deformation methods. *Agric For Meteorol* 150:1046–1056.
- Sun H, Aubrey DP, Teskey RO (2012) A simple calibration improved the accuracy of the thermal dissipation technique for sap flow measurements in juvenile trees of six species. *Trees* 26:631–640.
- Tateshi M, Kumagai T, Utsumi Y, Umebayashi T, Shiiba Y, Inoue K, Kaji K, Cho K, Otsuki K (2008) Spatial variations in xylem sap flux density in evergreen oak trees with radial-porous wood: comparisons with anatomical observations. *Trees* 22:23–30.
- Taylor AM, Gartner BL, Morrell JJ (2002) Heartwood formation and natural durability—a review. *Wood Fiber Sci* 34:587–611.
- Tyree MT, Zimmerman MH (2002) *Xylem structure and the ascent of sap*. Springer, Berlin, pp 229–239.
- von Allmen EI, Sperry JS, Smith DD, Savage VM, Enquist BJ, Reich PB, Bentley LP (2012) A species-level model for metabolic scaling of trees II. Testing in a ring- and diffuse-porous species. *Funct Ecol* 26:1066–1076.
- Warton DI, Wright IJ, Falster DS, Westoby M (2006) Bivariate line-fitting methods for allometry. *Biol Rev* 81:259–291.
- West GB, Brown JH, Enquist BJ (1999) A general model for the structure and allometry of plant vascular systems. *Nature* 400:664–667.
- Wullschleger SD, King AW (2000) Radial variation in sap velocity as a function of stem diameter and sapwood thickness in yellow-poplar trees. *Tree Physiol* 20:511–518.
- Wullschleger SD, Meinzer FC, Vertessy RA (1998) A review of whole-plant water use studies in tree. *Tree Physiol* 18:499–512.
- Yang KC, Hazenberg G (1991) Sapwood and heartwood width relationship to tree age in *Pinus banksiana*. *Can J For Res* 21:521–525.